Journal of Organometallic Chemistry 824 (2016) 7–14

Contents lists available at ScienceDirect

Journal of Organometallic Chemistry

journal homepage: www.elsevier.com/locate/jorganchem

Palladium complexes catalyzed regioselective arylation of 2-oxindole *via in situ* C(sp^2)–OH activation mediated by PyBroP

A. Vignesh [a], Werner Kaminsky [b], N. Dharmaraj [a, *]

[a] Inorganic & Nanomaterials Research Laboratory, Department of Chemistry, Bharathiar University, Coimbatore 641 046, India
[b] Department of Chemistry, University of Washington, Seattle, WA 98195, USA

ARTICLE INFO

Article history:
Received 5 July 2016
Received in revised form
1 September 2016
Accepted 29 September 2016
Available online 30 September 2016

Keywords:
Pd(II) complexes
C(sp^2)–OH activation
Aqueous-organic media
Room-temperature

ABSTRACT

Pd(II) complexes appended with ONO pincer type ligand were synthesized, structurally characterized and successfully applied as catalysts for regieoselective C–2 arylation of 2-oxindole *via in situ* C (sp^2)–OH activation in aqueous-organic media under an open atmosphere at room-temperature. This catalyst was reused up to four cycles. Favourably, the present protocol doesn't require the addition of any external oxidant, additives or phase transfer agents.

1. Introduction

Tautomerizable heterocycles are most suitable synthons in molecular engineering [1] and have been used as substrates for Pd-catalyzed cross-couplings *via in situ* C–OH activation in the presence of phosphonium salts. In this context, Kang et al. [2] reported direct arylation of tautomerizable heterocycles utilizing boronic acids as coupling accomplice. Herein, we demonstrate bromo-tris-pyrrolidino-phosphonium hexafluorophpsphate (PyBroP) mediated C–OH activation methodology [3] for arylation of 2-oxindole in the presence of palladium pincer type complex. Indole and its derivatives present as one of the main constituents of many natural and synthetic compounds exhibit medicinal [4] as well as material properties applicable to organic photovoltaics [5], OLED [6], sensors [7], nanomaterials [8], and forming useful coordination complexes [9].

Known synthetic routes so far developed to synthesize, for example, C-2 arylated indole derivatives exclude C–OH activation [10]. In addition, those methods require high catalyst loading, elevated temperature, prolonged reaction time, additives, oxidants, and usually require to work in a nitrogen atmosphere. It should be noticed that aromatic Csp^2–OH activation is profoundly difficult when compared to activating Csp^3–OH bonds because of a higher energy barrier and aromatic ring stability [11]. This C–OH activation methodology creates C–O electrophiles are considered a suitable alternative to aryl halides in C–C bond formation reactions [12].

For this reason, a series of aryl C–O electrophiles like acetates [13], carbamates [14], esters [15], ethers [16], pivalates [17], phosphoramides [18], phosphonates [19], triflates [19], sulfamates [20], carbonates [21], and tosylates [22] were introduced as coupling partners in metal-catalyzed cross-coupling reactions. Very recently, PyBroP mediated C–OH activation in the presence of metal catalysts has attracted the attention of several researchers. So far, PyBroP mediated C–OH activation was reported for urea [11], phenol [23], 1-naphthol [24], 2-quinoxalinone [2], 2-methyl-1H-pyridazine-3,6-dione [25], 2-hydroxypyridine [26], 2-oxoquninoline [27], and 2(1H)-pyrazinones [28] in the literature. Palladium based pincer complexes are widely utilized as catalysts for various organic reactions including C–H activation and they undoubtedly play a vital role in the continuous search for the development of new and efficient protocols to form C–C bonds [29]. Some of these complexes are workable in aqueous or aqueous-organic media [30]. We already examined palladium pincer type complexes as catalysts for organic reactions [31]. We herein report the synthesis and spectral characterization of three new palladium (II) complexes (**1**–**3**) bearing ONO pincer type ligands including X-

* Corresponding author.
E-mail address: dharmaraj@buc.edu.in (N. Dharmaraj).
URL: http://ndharmaraj.wix.com/inrl

http://dx.doi.org/10.1016/j.jorganchem.2016.09.026
0022-328X/

ray structures, and studies of their catalytic activity towards C-2 arylation of 2-oxindole using substituted aryl boronic acids in H_2O/EtOH media under open-flask conditions.

2. Experimental procedure

2.1. General information

Elemental analyses (C, H, and N) were performed on a Vario EL III Elemental analyzer instrument. IR spectra (4000–400 cm^{-1}) were recorded on a Nicolet Avatar Model FT-IR spectrophotometer. Melting points were determined with a Lab India instrument. ^1H and ^{13}C NMR spectra were recorded in deuterated $CHCl_3$ as solvent on BRUKER 400 and 100 MHZ instruments, respectively. All reagent grade chemicals were used without further purification unless otherwise specifically mentioned. Solvents were purified and dried according to standard procedures [32].

2.2. Synthesis of ligands H_2L1– H_2L3

The pincer type ligands H_2L1–H_2L3 were synthesized from equimolar quantity of *o*-hydroxynaphthaldehyde with appropriate hydrazides such as benzhydrazide (H_2L1), *p*-chlorobenzhydrazide (H_2L2), and *p*-nitrobenzhydrazide (H_2L3) in ethanol according to a literature method [33]. The reaction mixture was then refluxed on a water-bath for 6 h and poured into crushed ice. The corresponding pincer type hydrazones formed as colorless solid were filtered, washed repeatedly with distilled water and recrystallized from ethanol with 80–90% yield. The purity of the ligands were checked by various analytical techniques and is in accordance with literature report [33].

2.3. General method for the synthesis of the palladium complexes

To a warm methanolic solution (20–30 mL) of appropriate ligands (H_2L1–H_2L3) (1 equiv.) was added a chloroform solution of [$PdCl_2(PPh_3)_2$] (1 equiv.) followed by two drops of triethylamine. Then the reaction mixture was refluxed for 8–10 h and kept at room temperature for crystallization. Needle like reddish brown crystals suitable for X-ray studies were obtained on slow evaporation over 45–60 days.

[Pd(L1) (PPh_3)] (complex **1**) Yield: 85% (112 mg). M. p. 232–234 °C. Elemental analysis (%) calculated for $C_{36}H_{27}N_2O_2PPd$; C, 65.81; H, 4.14; N, 4.26. Found (%) C, 65.82; H, 4.15; N, 4.27. UV–visible (solvent: DMSO, nm): 303, 325, 341, 354. Selected IR bands (KBr, ν in cm^{-1}): 1581 (C–N=N–C), 1528 (C=N), 1433 (PPh_3), 1260 (imidolate –N=C–O), 1185 (naphtholate C–O). ^1H NMR ($CDCl_3$, δ ppm) 9.86 (s, 1H), 9.30 (d, J = 8 Hz, 4H), 7.81 (s, 2H), 7.55 (d, J = 7.6 Hz, 2H), 7.23–7.36 (m, 10H), 7.15 (t, J = 5.8 Hz, 6H), 6.44 (d, J = 15.6 Hz, 2H); ^{13}C NMR ($CDCl_3$, δ ppm) 183.5, 167.5, 145.2, 142.2, 138.5, 134.7, 129.4, 128.3, 127.0, 124.4, 123.9, 120.7, 119.3, 118.4, 112.0.

[Pd(L2) (PPh_3)] (complex **2**) Yield: 80% (111 mg). M. p. 239–242 °C. Elemental analysis (%) calculated for $C_{36}H_{26}ClN_2O_2PPd$; C, 62.53; H, 3.79; N, 4.05. Found (%) C, 62.52; H, 3.78; N, 4.05. UV–visible (solvent: DMSO, nm): 306, 329, 342, 353. Selected IR bands (KBr, ν in cm^{-1}): 1591(C–N=N–C), 1526 (C=N), 1429 (PPh_3), 1267 (imidolate –N=C–O), 1184 (naphtholate C–O), 745 (C–Cl). ^1H NMR ($CDCl_3$, δ ppm): H^1 NMR: 9.86 (s, 1H), 9.16 (d, J = 12.0 Hz, 2), 7.73 (s, 2H), 7.65 (s, 2H), 7.48 (s, 2H), 7.38 (t, J = 6.0 Hz, 9H), 7.18 (t, J = 3.8 Hz, 6H), 6.43 (d, J = 16.0 Hz, 2H); ^{13}C NMR ($CDCl_3$, δ ppm) 183.2, 167.0, 143.7, 142.2, 139.5, 134.2, 131.1, 129.4, 128.7, 127.3, 123.9, 123.3, 120.1, 119.7, 117.7, 114.6.

[Pd(L3) (PPh_3)] (complex **3**) Yield: 88% (124 mg). M. p. 246–248 °C. Elemental analysis (%) calculated for $C_{36}H_{26}N_3O_4PPd$; C, 61.59; H, 3.73; N, 5.99. Found (%) C, 61.58; H, 3.74; N, 5.98. UV–visible (solvent: DMSO, nm): 302, 323, 344, 369. Selected IR bands (KBr, ν in cm^{-1}): 1590 (C–N=N–C), 1526 (C=N), 1477 (NO_2), 1433 (PPh_3), 1249 (imidolate –N=C–O), 1186 (naphtholate C–O). ^1H NMR ($CDCl_3$, δ ppm): H^1 NMR: 9.65 (s, 1H), 9.55 (d, J = 16.0 Hz, 2H), 7.62 (d, J = 6.4 Hz, 3H), 7.52 (t, J = 7.4 Hz, 3H), 7.46 (t, J = 7.4 Hz, 5H), 7.40 (d, J = 6.8 Hz, 2H), 7.25–7.30 (m, 5H), 6.94 (t, J = 3.8 Hz, 2H), 6.44 (d, J = 16 Hz, 3H). ^{13}C NMR ($CDCl_3$, δ ppm) 185.6, 155.8, 154.7, 138.1, 135.6, 130.7, 130.3, 129.2, 128.9, 128.8, 128.7, 127.8, 125.7, 124.5, 124.4, 121.8, 117.1, 113.3.

2.4. Single-crystal X-ray diffraction studies

Suitable crystals of complexes **1**–**3** with approximate dimensions of 0.24 × 0.15 x 0.10, 0.30 × 0.10 x 0.03 and 0.17 × 0.15 × 0.05 mm^3 were mounted on a loop with oil. The data collection were performed by using Bruker APEX II single crystal X-ray diffractometer. All the data were collected using graphite monochromated Mo Kα radiation (λ = 0.71073 Å) from a fine focus sealed tube X-ray source. The collected data were integrated and scaled using hkl-SCALEPACK [34] (for complex **1**) and SAINT, SADABS within the APEX2 software package by Bruker [35] (for complex **2**, and **3**). While using hkl-SCALEPACK program applies a multiplicative correction factor (S) to the observed intensities (I) and has the following form:

$$S = \left(e^{-2B(\sin^2\theta)/\lambda^2}\right)/\text{scale}$$

S is calculated from the scale and the B factor determined for each frame and is then applied to I to give the corrected intensity (I_{corr}). Solution by direct methods (SHELXS, SIR97) [36] produced a complete heavy atom phasing models consistent with the proposed structures. The structure was completed by difference Fourier synthesis with SHELXL97 [37,38]. The scattering factors are from Waasmair and Kirfel [39] Hydrogen atoms were placed in geometrically idealized positions and constrained to ride on their parent atoms with C–H distances in the range 0.95–1.00 Å. Isotropic thermal parameters Ueq were fixed such that they were 1.2 Ueq of their parent atom Ueq for CH's and 1.5 Ueq of their parent atom Ueq in case of methyl groups. All non-hydrogen atoms were refined anisotropically by full-matrix least-squares.

2.5. General procedure for catalytic reaction and reusability

To a mixture of H_2O–EtOH (70:30%), 2-oxindole (3.0 mmol), NEt_3 (6.0 equiv) and PyBroP (1.2 equiv.) were added and stirred for 10 min. To this reaction mixture, complex 3 (0.01 mol) was added and stirred for 30 min at room-temperature followed by the addition of KOH (5 mmol) and phenylboronic acid (4.0 mmol). The progress of the reaction was monitored by thin layer chromatography (TLC). After the completion of the reaction the product mixture was cooled to room temperature; the catalyst was precipitated by the addition of ethyl acetate separated by centrifugation and washed thoroughly with water (to remove inorganic salts). The identity of the products was confirmed by ^1H and ^{13}C NMR techniques. The recovered catalyst was dried and utilized for next cycle under same reaction conditions. The stability of recovered catalyst was identified by ^1H, ^{31}P NMR spectra, melting point data and R_f value of TLC.

3. Results and discussion

Palladium complexes of the composition [Pd (L1–L3) (PPh_3)] were synthesized by reacting equimolar quantity of [$PdCl_2(PPh_3)_2$]

and respective aryl hydrazones (H_2L1–H_2L3) *via* metal introduction route as depicted in Scheme 1. The chosen hydrazones are suitable to provide three donor atoms *i.e.* two oxygen atoms and a nitrogen atom to form pincer type palladium complexes.

FT-IR spectra of free ligands H_2L1- H_2L3 displayed medium bands at 3410, 3412 and 3430 cm^{-1} respectively, due to the presence of O–H group in naphthalene ring. A strong band observed at 3052, 3098 and 3110 cm^{-1} confirmed the presence of N–H functional group in the free ligands. The absorption due to C=O stretching was observed at 1632, 1631 and 1642 cm^{-1}. IR spectra of the palladium complexes **1**–**3** did not show any bands due to N–H and C=O functional groups. Absence of these bands indicates that the ligands underwent tautomerization followed by deprotonation prior to coordination of the imidolate oxygen to palladium (II) ion. Further, the new bands appeared in the regions of 1181–1186 cm^{-1} and 1590-1610 cm^{-1} were attributed to the C–O and C–N=N–C fragments of the coordinated ligand. The spectra of complexes **1**–**3** showed a strong band at 1482, 1431 and 1477 cm^{-1} to reveal the presence of PPh_3. From the above discussions, the coordination of pincer type hydrazone ligands *via* naphtholate oxygen, azomethine nitrogen, and imidolate oxygen to palladium ion were identified [40].

The proton NMR spectra of complexes **1**–**3** registered a downfield resonance of sharp singlets at δ 9.86, 9.86, and 9.65 respectively due to azomethine proton. All the aromatic protons of the complexes **1**–**3** displayed their resonances in the region of δ 6.42–9.55 ppm. It's important to note here that we didn't observe any signal due to N–H proton which indicated that the enolization of carbonyl oxygen followed by its coordination to palladium ion in the imidolate form. Also, the non-existence of a resonance attributable to the O–H group attached to naphthalene ring revealed that there occurred a deprotonation prior to its coordination to palladium ion in the complexes **1**–**3** [41]. The ^{13}C NMR spectra of all the Pd(II) complexes showed a downfield shift in the position of azomethine carbon (C=N) compared to free ligands and appeared at δ 183.5, 183.2 and 185.6 ppm. The signals corresponding to imidolate carbon atom (N=C–O) appeared at δ 167.5, 167.0 and 155.8. In addition, the ^{13}C NMR spectra of all the Pd(II) complexes displayed signals in the region of δ 111.3–149.1 ppm due to various aromatic carbon atoms of both hydrazone and triphenyl phosphine moieties [42].

Single-crystal XRD of complexes **1**–**3** show that pincer type ligands (H_2L1– H_2L3) adopt to the palladium ion in a binegative tridentate manner. The naphtholate oxygen, azomethine nitrogen and the deprotonated imidol oxygen act as three donor atoms and each forma five membered and a six membered chelate ring with

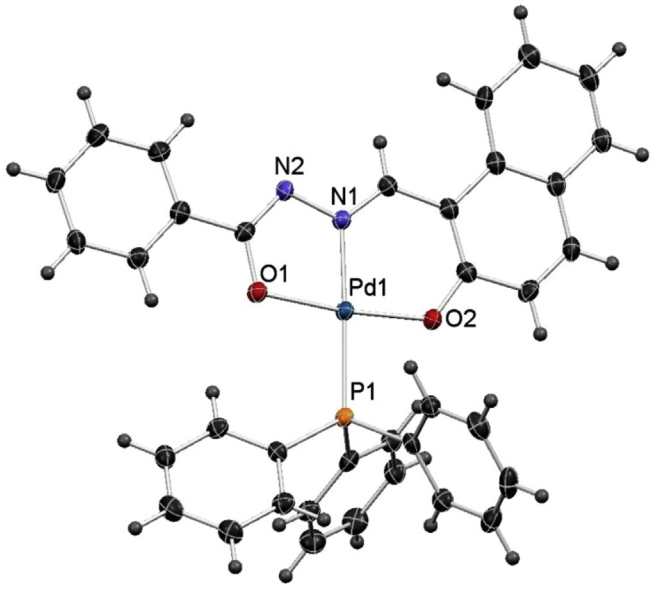

Fig. 1. ORTEP diagram of complex **1** with thermal ellipsoids at the 50% probability level.

the palladium ion, while the fourth coordination site is occupied by a triphenylphosphine molecule. The geometry around the Pd(II) centre in complexes **1**–**3** is best described as distorted square-planar. ORTEP representations of complexes **1**–**3** are shown in Figs. 1–3. The observed bond lengths and bond angles are in good agreement with reported data on related palladium (II) complexes [43]. Crystal data, structure refinement selected bond distances and bond angles of the complexe **1**–**3**, were gathered in Tables 1–4.

To establish the feasibility of direct arylation of 2-oxindole in a regioselective manner, we applied Kang et al. [2], conditions using 2-oxindole and phenylboronic acid as model substrates in presence of PyBroP and complex **2** as catalyst. As expected, the reaction proceeded but to afford only 17% of the desired product. In order to increase the yield of desired product, we examined diverse solvents, bases and catalysts. Initially, we tried this reaction in water wherein no reaction was observed owing to the insoluble nature of the catalyst (Table 5, entry 1). Hence, we conducted the same experiment by including some organic solvents to dissolve the catalyst. To identify a most suitable solvent for this catalytic process, combinations of MeOH, THF, EtOAc, DMF, CH_3CN, DMSO, EtOH, toluene, benzene, $CHCl_3$ and DCM solvents with water were

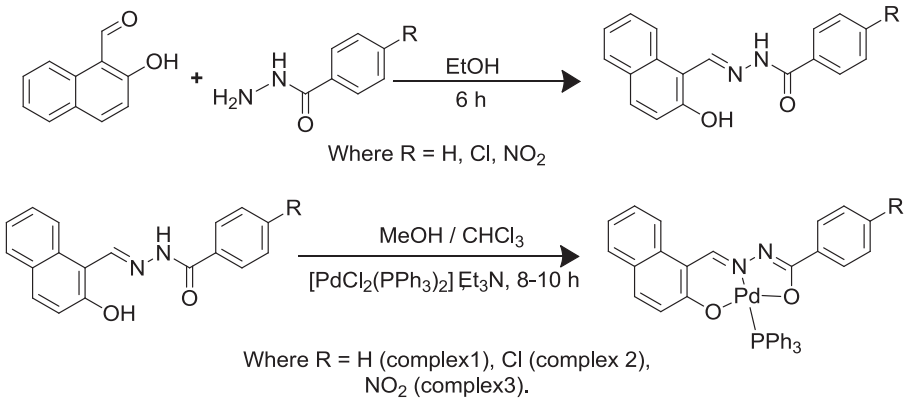

Scheme 1. Synthesis of ONO pincer type ligands and their Pd(II) Complexes.

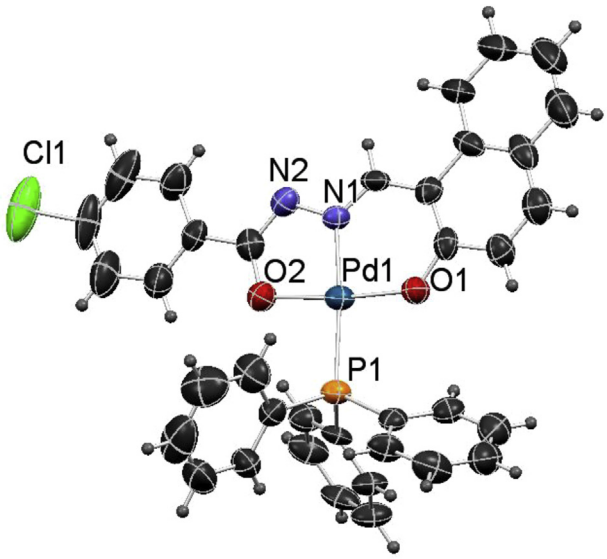

Fig. 2. ORTEP diagram of complex **2** with thermal ellipsoids at the 50% probability level.

tested. Next, we studied the role of various bases such as KOH, K_2CO_3, NaOH, Na_2CO_3, Et3N and pyridine. The outcome of the above trials regarding the choice of solvent and base suggested that utilizing KOH as a base with a H_2O/EtOH solvent mixture produced 84% of the arylated indole while any other combination of solvents gave less product (Table 5). The comparison of catalytic potential of the complexes **1**, **2** and **3** were examined as well. Among those, complex **3** exhibited the best performance for the reaction to afford 94% isolated yield (Table 5, entry 26). The presence of an electron withdrawing $-NO_2$ in the pincer type ligand coordinated to Pd ion in complex **3** may be the reason for the excellent performance of this complex [44]. Thus, the following conditions were utilized: 2-oxindole (3 mmol), aryl boronic acid (4 mmol) KOH (5, mmol), Et_3N (6 eqv.), PyBroP (1.2 eqv.), H_2O/EtOH (70:30%), and complex **3** as catalyst (0.01 mol %); all at room-temperature.

The scope of catalytic activity was examined at above optimized conditions on a series of aryl boronic acids decorated by both, electron-rich or electron-deficient groups (Table 6). Within the

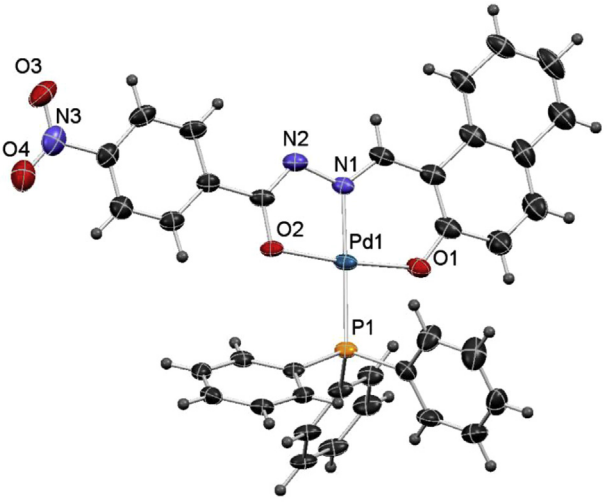

Fig. 3. ORTEP diagram of complex **3** with thermal ellipsoids at the 50% probability level.

Table 1
Selected bond lengths (Å) and angles (°) for the complex **1**.

Complex	1
N (1)–Pd (1)	1.9680 (3)
O (1)–Pd (1)	1.9890 (2)
O (2)–Pd (1)	1.9680 (2)
P (1)–Pd (1)	2.2922 (10)
C (11)–N (1)	1.2980 (4)
C (12)–N (2)	1.3040 (5)
C (12)–O (1)	1.3200 (4)
C (1)–O (2)	1.3180 (4)
N (1)–N (2)	1.4000 (4)
C (10)–C (11)	1.4360 (5)
C (1)–C (10)	1.4050 (5)
N (1) – Pd (1) – O (1)	80.10 (11)
O (2) – Pd (1) – N (1)	93.75 (11)
O (1) – Pd (1) – O (2)	173.77 (10)
N (1) – Pd (1) – P (1)	177.91 (9)
O (1) – Pd (1) – P (1)	98.42 (8)
O (2) – Pd (1) – P (1)	87.76 (8)
C (11) – N (1) – Pd (1)	125.90 (2)
N (2) – C (12) – O (2)	125.10 (3)
N (2) – N (1) – Pd (1)	115.30 (2)

Table 2
Selected bond lengths (Å) and angles (°) for the complex **2**.

Complex	2
N (1)–Pd (1)	1.976 (5)
O (1)–Pd (1)	1.952 (4)
O (2)–Pd (1)	2.001 (4)
P (1)–Pd (1)	2.2936 (18)
C (8)–N (1)	1.284 (6)
C (1)–N (2)	1.312 (7)
C (1)–O (2)	1.328 (7)
C (18)–O (1)	1.320 (7)
N (1)–N (2)	1.402 (6)
C (8)–C (9)	1.412 (8)
C (9)–C (18)	1.424 (9)
N (1) – Pd (1) – O (1)	92.9 (2)
O (2) – Pd (1) – N (1)	81.2 (2)
O (1) – Pd (1) – O (2)	174.04 (19)
N (1) – Pd (1) – P (1)	174.70 (15)
O (1) – Pd (1) – P (1)	92.31 (13)
O (2) – Pd (1) – P (1)	93.62 (15)
C (8) – N (1) – Pd (1)	126.5 (4)
N (2) – C (1) – O (2)	125.1 (6)
N (2) – N (1) – Pd (1)	113.9 (4)

Table 3
Selected bond lengths (Å) and angles (°) for the complex **3**.

Complex	3
N (1)–Pd (1)	1.974 (3)
O (1)–Pd (1)	1.961 (3)
O (2)–Pd (1)	1.981 (2)
P (1)–Pd (1)	2.2825 (9)
C (11)–N (1)	1.2940 (5)
C (12)–N (2)	1.3040 (5)
C (1)–O (1)	1.308 (4)
C (12)–O (2)	1.321 (4)
N (1)–N (2)	1.400 (4)
C (10)–C (11)	1.424 (6)
C (1)–C (10)	1.420 (5)
N (1) – Pd (1) – O (1)	93.61 (11)
O (2) – Pd (1) – N (1)	80.34 (11)
O (1) – Pd (1) – O (2)	173.91 (9)
N (1) – Pd (1) – P (1)	176.27 (9)
O (1) – Pd (1) – P (1)	88.71 (8)
O (2) – Pd (1) – P (1)	97.37 (7)
C (11) – N (1) – Pd (1)	126.2 (3)
N (2) – C (12) – O (2)	125.9 (4)
N (2) – N (1) – Pd (1)	115.1 (2)

Table 4
Crystal data and structure refinement for complexes **1**, **2** and **3**.

Complex	1 (R = H)	2 (R = Cl)	3 (R = NO_2)
CCDC number	1022416	1022419	1022417
Empirical formula	C_{36} H_{27} N_2 O_2 P Pd	C_{36} H_{26} Cl N_2 O_2 P Pd	C_{36} H_{26} N_3 O_4 P Pd
Formula weight	657.02	691.41	701.97
Temperature (K)	130 (2)	292 (2)	100 (2)
Wavelength (Å)	0.71073	0.71073	0.71073
Crystal system	Monoclinic	Monoclinic	Triclinic
Space group	P 2_1/n	P 2_1/c	P −1
Unit cell dimensions			
a (Å)	15.7562 (5)	8.9410 (15)	8.8556 (4)
b (Å)	8.8280 (3)	23.823 (4)	14.9323 (11)
c (Å)	20.6955 (8)	30.581 (6)	15.0168 (7)
α (°)	90	90	60.333 (3)
β (°)	97.0600 (10)	93.790 (4)	80.889 (3)
γ (°)	90	90	78.713 (5)
Volume ($Å^3$)	2856.83 (17)	6500 (2)	1687.66 (17)
Z	4	8	2
Density (calculated) (Mg m^{-3})	1.528 Mg/m^3	1.413	1.381
Absorption coefficient (mm^{-1})	0.743	0.736	0.639
F (000)	1336	2800	712
Crystal size (mm^3)	0.24 × 0.15 x 0.10	0.30 × 0.10 x 0.03	0.17 × 0.15 x 0.05
Reflections collected	11566	54110	86402
Independent reflections	6731 [R (int) = 0.0647]	16017 [R (int) = 0.1415]	8389 [R (int) = 0.0613]
Max. and min. transmission	0.9294 and 0.8419	0.9782 and 0.8093	0.9688 and 0.8992
Refinement method	Full-matrix least-squares on F^2	Full-matrix least-squares on F^2	Full-matrix least-squares on F^2
Data/restraints/parameters	6731/0/382	16017/0/775	8389/0/406
Goodness-of-fit on F^2	0.983	0.781	1.052
Final R indices [I > 2σ(I)]	R1 = 0.0500, wR2 = 0.1225	R1 = 0.0655, wR2 = 0.0990	R1 = 0.0547, wR2 = 0.1215
R indices (all data)	R1 = 0.0767, wR2 = 0.1367	R1 = 0.2165, wR2 = 0.1303	R1 = 0.0818, wR2 = 0.1299
Largest diff. peak and hole (e.$Å^{-3}$)	1.491 and −1.304	0.563 and −0.469	0.572 and −1.051

selected compounds, aryl boronic acids featuring strongly activating groups such as $-OCH_3$, and $-OH$ gave significant yields (Table 6, entries 6e, 6f, and 6i). Remarkably, a boronic acid with high steric hindrance *i.e.*, 2, 6-dimethoxyphenylboronic acid utilized in the reaction gave 70% of the desired product (Table 6, entry 6 g). Successfully, naphthyl and biphenyl boronic acids were also smoothly converted into desired arylated indoles (Table 6, entries 6j and 6k). Likewise, aryl boronic acids possessing *m*−Cl, *p*−Br, and *p*−$N(CH_3)_2$ groups underwent the reaction smoothly to afford the expected products in good yields (Table 6, entries 6l, 6 m, and 6n). It is significant to note that the presence of halogens (bromo/chloro) in the arylated indoles possess an additional advantage (Table 6, entries 6l and 6 m) as they are suitable for further functionalization through cross coupling. However, aryl boronic acids bearing alkyl groups like *p* −*t*-butyl, and $-CH_3$ group at either *ortho* or *para* as well as at both *ortho* and *meta* positions gave 82, 90, 92, and 89% yields, respectively (Table 6, entries 6h, 6b, 6c, and 6d).

Moderately deactivating groups like acetyl or formyl, occupying the *meta* and *para* position of phenylboronic acids, were well tolerated under the reaction conditions to afford the desired coupling product (Table 6, entries 6°, 6p and 6q). Moreover, a phenylboronic acid with deactivating $-CF_3$ group in the *para* position also reacted smoothly to give the corresponding arylated product (Table 6, entry 6r). Based on the above observations, reacting indoles with electron-rich aryl boronic acids is more feasible than with others.

In order to prove the efficacy of this catalytic methodology for industrial application, we tested the gram scale synthesis of 2-phenyl-3-*H*-indole (6a) as a representative example wherein (Scheme 2) 82% yield of the product was realized.

To screen the reusability, the selected catalyst 3 was utilized under parallel reaction conditions. The first cycle afforded 94% of the corresponding coupled product followed by 88% in the next run. However, third and fourth cycles gave 80% and 69% of the coupled product. The lower yield observed after the fourth cycle

Table 5
Optimization of cross-coupling Conditions[a]

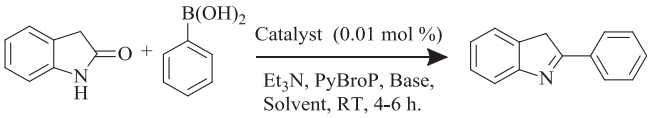

Entry	Catalyst	Base	Solvent	Yield (%)[b]
1	Complex 2	No base	H_2O	NR[c]
2	Complex 2	No base	H_2O/MeOH	12
3	Complex 2	KOH	H_2O/MeOH	76
4	Complex 2	K_2CO_3	H_2O/MeOH	69
5	Complex 2	NaOH	H_2O/MeOH	66
6	Complex 2	Na_2CO_3	H_2O/MeOH	60
7	Complex 2	Et_3N	H_2O/MeOH	37
8	Complex 2	Pyridine	H_2O/MeOH	32
9	Complex 2	KOH	H_2O/THF	52
10	Complex 2	KOH	H_2O/EtOA[c]	49
11	Complex 2	KOH	H_2O/DMF	56
12	Complex 2	KOH	H_2O/CH_3CN	44
13	Complex 2	KOH	H_2O/DMSO	51
14	Complex 2	KOH	H_2O/MeOH	76
15	Complex 2	KOH	H_2O/EtOH	84
16	Complex 2	KOH	H_2O/toluene	55
17	Complex 2	KOH	H_2O/benzene	53
18	Complex 2	KOH	H_2O/$CHCl_3$	45
19	Complex 2	KOH	H_2O/DCM	32
20	Complex 2	KOH	H_2O/EtOH (10%)	68
21	Complex 2	KOH	H_2O/EtOH (20%)	72
22	Complex 2	KOH	H_2O/EtOH (30%)	84
23	Complex 2	KOH	H_2O/EtOH (40%)	76
24	Complex 2	KOH	H_2O/EtOH (50%)	70
25	Complex 1	KOH	H_2O/EtOH (30%)	79
26	**Complex 3**	**KOH**	**H_2O/EtOH (30%)**	**94**

Bold implies the optimization of the reaction conditions.
[a] Reaction conditions: 2-oxindole (3 mmol), phenylboronic acid (4 mmol), base (5, mmol), Et_3N (6 eqv.), PyBroP (1.2 eqv.) solvent (80:20%) and catalyst (0.01 mol %) stirred at room temperature for 4–6 h.
[b] Isolated yield.
[c] No reaction.

Table 6
Cross-coupling of 2-oxindole and various aryl boronic acids (6a–6r) under optimized reaction conditions.[a]

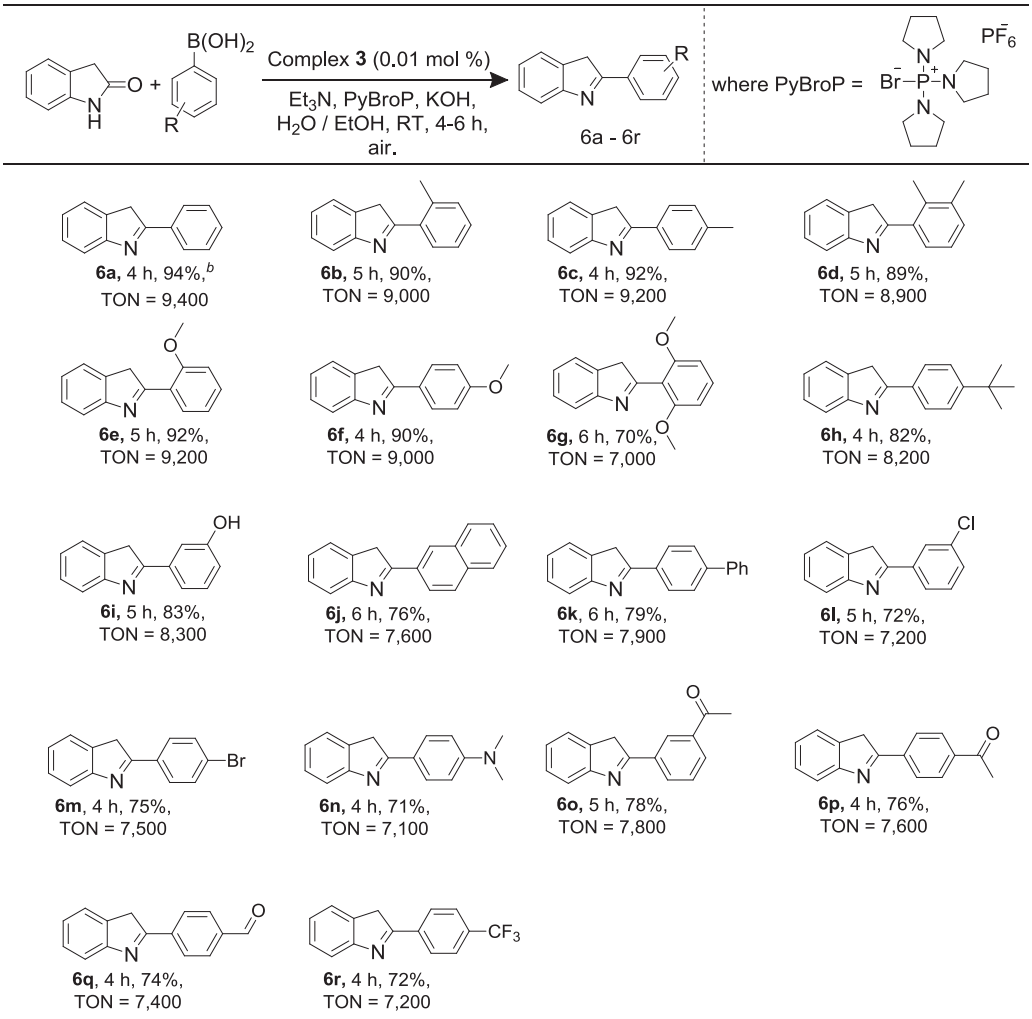

[a] = Reaction conditions: 2-oxindole (3 mmol), aryl boronic acid (4 mmol), KOH (5, mmol), Et_3N (6 eqv.), PyBroP (1.2 eqv.) H_2O/EtOH (70:30%) and catalyst (0.01 mol %) stirred at room temperature for 4-6 h. TON = Turnover number = ratio of moles of product formed to moles of catalyst used. [b] = Isolated yield.

may be due to decomposition of the catalyst to leach out palladium. The overall result of the reusability experiment is summarized in Fig. 4. The stability of recovered catalyst was identified by ^{1}H NMR spectra, melting point data and R_f value of TLC. The detailed recovery process is provided in experimental section. The ^{1}H NMR spectrum of the used catalyst recovered from the first catalytic cycle confirmed that the pincer structure of complex 3 remained intact.

Based on previous reports [2,31,45–47], a plausible mechanism for C–OH activation is proposed in Scheme 3. Initially, $Pd^{(0)}L$ (**I**)

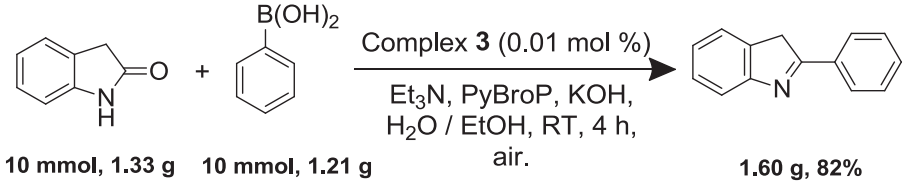

Scheme 2. Gram scale synthesis of 2-phenyl-3-*H*-indole (6a).

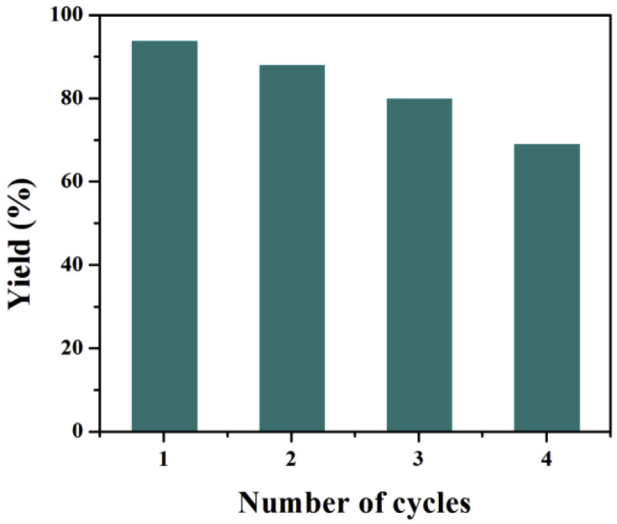

Fig. 4. Reusability of catalyst **3**.

formed through a two-electron reduction of the starting palladium (II) complex in presence of a base [45]. The phosphonium salt intermediate **I** obtained by the activation of indol-2-ol with PyBroP enters into the Pd $^{(0)}$L catalytic cycle *via* oxidative addition to give intermediate **II**. Addition of KOH to intermediate **II** gave an intermediate III through metathetic process. Transmetalation of intermediate **III** with phenylboronic acid provides intermediate **IV**, which undergoes reductive elimination to afford 2-phenylindole with regeneration of the Pd $^{(0)}$L. Finally, oxidation of active species Pd$^{(0)}$ L by O_2 led to the catalyst Pd$^{(II)}$L [46,47].

4. Conclusions

First report on the arylation of 2-oxindole with aryl boronic acids *via* PyBroP mediated *in situ* C (sp^2)–OH activation catalyzed by Pd(II) pincer type complexes in H_2O/EtOH mixture at room-temperature. All the palladium complexes were characterized by IR, ^{1}H, ^{13}C NMR and single-crystal X-ray diffraction. The current strategy afforded 94% of the coupled product in a highly region-selective manner with the catalyst the reusable up to four cycles.

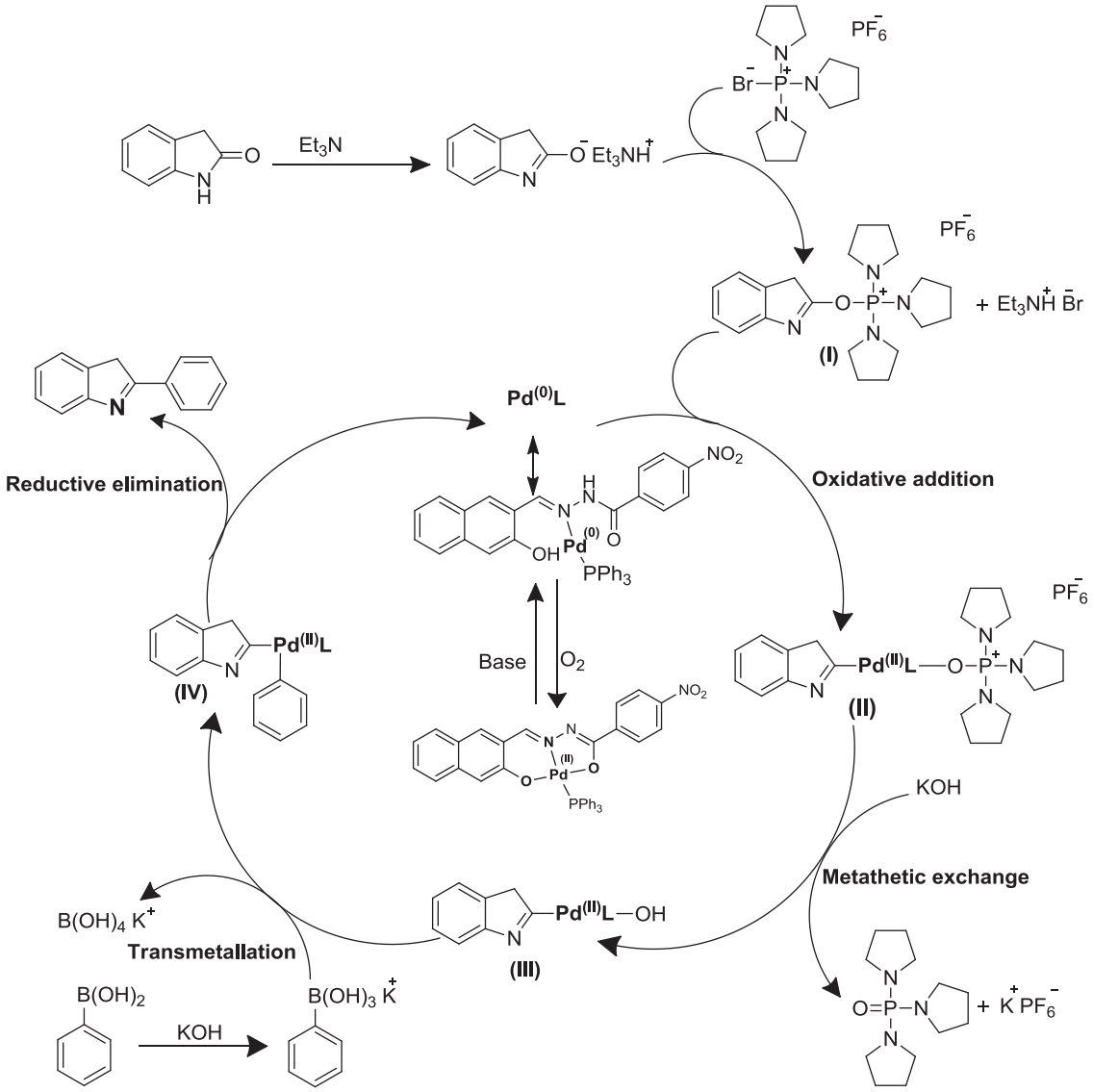

Scheme 3. Proposed mechanism for arylation of 2-oxindole.

Hence, the present palladium catalyzed methodology could be considered as an attractive route to synthesize a series of biologically active 2-arylindoles in excellent yield.

Acknowledgements

Mr. A. Vignesh thanks the University Grants Commission (UGC), New Delhi, India. for the award of Senior Research Fellowship (SRF) under UGC-BSR RFSMS.

Appendix A. Supplementary data

Supplementary data related to this article can be found at http://dx.doi.org/10.1016/j.jorganchem.2016.09.026.

References

[1] The Merck Index, An Encyclopedia of Chemicals, Drugs and Biologicals, 3th ed., Merck & Co., Inc., Whitehouse Station, NJ, 2001.
[2] a) F.A. Kang, Z. Sui, W.V. Murray, J. Am. Chem. Soc. 130 (2008) 11300;
b) F.A. Kang, C. James, J.C. Lanter, C. Cai, Z. Sui, W.V. Murray, Chem. Commun. 46 (2010) 1347.
[3] a) G. Tan, T. Szilvasi, S. Inoue, B. Blom, M. Driess, J. Am. Chem. Soc. 136 (2014) 9732.
[4] V. Sharma, P. Kumar, D. Pathak, J. Heterocycl. Chem. 47 (2010) 491.
[5] Z.K. Owczarczyk, W.A. Braunecker, A. Garcia, R. Larsen, A.M. Nardes, N. Kopidakis, D.S. Ginley, D.C. Olson, Macromolecules 46 (2013) 1350.
[6] M.S. Park, D.H. Choi, B.S. Lee, J.Y. Lee, J. Mater. Chem. 22 (2012) 3099.
[7] P.A. Gale, Chem. Commun. (2008) 4525.
[8] J. Nanda, A. Biswas, B. Adhikari, A. Banerjee, Angew. Chem. Int. 52 (2013) 5041.
[9] A. González, J. Granell, C. López, R. Bosque, L.J. Rodríguez, J. Organomet. Chem. 726 (2013) 21.
[10] a) S.B. Lane, D. Sames, Org. Lett. 6 (2004) 2897;
b) Z. Liang, B. Yao, Y. Zhang, Org. Lett. (2010) 3185;
c) S.B. Lane, A.M. Brown, D. Sames, J. Am. Chem. Soc. 127 (2005) 8050;
d) C. Sollert, K. Devaraj, A. Orthaber, P.J. Gates, L.T. Pilarski, Chem. Eur. J. 21 (2015) 1;
e) G.S. Modha, F.M. Greaney, J. Am. Chem. Soc. 137 (2015) 1416;
f) S. Cacchi, G. Fabrizi, L.M. Parisi, Org. Lett. 5 (2003) 3843.
[11] J.P. Dalvadi, K.P. Patel, H.K. Chikhalia, Tetrahedron 70 (2014) 9394.
[12] (a) B.M. Rosen, K.W. Quasdorf, D.A. Wilson, N. Zhang, A.M. Resmerita, N.K. Garg, V. Percec, Chem. Rev. 111 (2011) 1346;
b) J. Yamaguchi, K. Muto, K. Itami, Eur. J. Org. Chem. 19 (2013);
(c) D.G. Yu, B.J. Li, Z.J. Shi, Acc. Chem. Res. 43 (2010) 1486.
[13] B.T. Guan, Y. Wang, B.J. Li, D.G. Yu, Z.J. Shi, J. Am. Chem. Soc. 130 (2008) 14468.
[14] a) M. Baghbanzadeh, C. Pilger, C.O. Kappe, J. Org. Chem. 76 (2011) 1507;
b) K.W. Quasdorf, M. Riener, K.V. Petrova, N.K. Garg, J. Am. Chem. Soc. 131 (2009) 17748;
c) K.W. Quasdorf, A.A. Finch, P. Liu, A.L. Silberstein, A. Komaromi, T. Blackburn, S.D. Ramgren, K.N. Houk, V. Snieckus, N.K. Garg, J. Am. Chem. Soc. 133 (2011) 6352.
[15] P. Leowanawat, N. Zhang, V. Percec, J. Org. Chem. 77 (2012) 1018.
[16] M. Tobisu, T. Shimasaki, N. Chatani, Angew. Chem. Int. 47 (2008) 4866.
[17] K.W. Quasdorf, X. Tian, N.K. Garg, J. Am. Chem. Soc. 130 (2008) 14422.
[18] Y.L. Zhao, Y. Li, L.X. Gao, F.S. Han, Chem. Eur. J. 16 (2010) 4991.
[19] H. Firouzabadi, N. Iranpoor, M. Gholinejad, A. Samadi, J. Mol. Catal. A Chem. 377 (2013) 190.
[20] G.J. Chen, F.S. Han, Eur. J. Org. Chem. (2012) 3575.
[21] K.W. Quasdorf, M. Riener, K.V. Petrova, N.K. Garg, J. Am. Chem. Soc. 131 (2009) 17748.
[22] H. Gao, Y. Li, Y.G. Zhou, F.S. Han, Y.J. Lin, Adv. Synth. Catal. 353 (2011) 309.
[23] N. Iranpoor, F. Panahi, Org. Lett. 17 (2015) 214.
[24] G.J. Chen, J. Huang, L.X. Gao, F.S. Han, F.S. Chem, Eur. J. 17 (2011) 4038.
[25] A. Sharma, D. Vachhani, E.V. Eycken, Org. Lett. 14 (2012) 1854.
[26] S.M. Li, J. Huang, G.J. Chena, F.S. Han, Chem. Commun. 47 (2011) 12840.
[27] S.Y. Kumar, C. Dasarathan, K. Prabakaran, F.R.N. Khan, E.D. Jeong, E.H. Chung, H.G. Kim, RSC Adv. 4 (2014) 40259.
[28] V.P. Mehata, S.G. Modha, E.V.V. Eycken, J. Org. Chem. 75 (2010) 976.
[29] a) D.B. Garagorri, K. Kirchner, Acc. Chem. Res. 41 (2008) 201;
b) N. Selander, K.J. Szabo, Chem. Rev. 111 (2011) 2048;
c) J.L. Niu, X.Q. Hao, J.F. Gong, M.P. Song, Dalton Trans. 40 (2011) 5135.
[30] a) A.K. Crawford, A.H. Cowley, S.M. Humphrey, Catal. Sci. Technol. 4 (2014) 1456;
b) W. Susanto, C.Y. Chu, W.J. Ang, T.C. Chou, L.C. Lo, Y. Lam, J. Org. Chem. 77 (2012) 2729;
c) H.D. Velazquezd, F. Verpoort, Chem. Soc. Rev. 41 (2012) 7032.
[31] a) A. Vignesh, W. Kaminsky, N.S.P. Bhuvanesh, N. Dharamraj, RSC Adv. 5 (2015) 59428;
b) A. Vignesh, W. Kaminsky, N. Dharmaraj, RSC Adv. 5 (2015) 77948;
c) A. Vignesh, W. Kaminsky, N. Dharmaraj, Green Chem. 18 (2016) 3295;
(d) A. Vignesh, W. Kaminsky, N. Dharmaraj, ChemCatChem (2016), http://dx.doi.org/10.1002/cctc.201600717.
[32] A.I. Vogel, Text Book of Practical Organic Chemistry, 5th ed., Longman, London, 1989.
[33] P. Sathyadevi, P. Krishnamoorthy, R.R. Butorac, A.H. Cowley, N.S.P. Bhuvanesh, N. Dharmaraj, Dalton Trans. 40 (2011) 9690.
[34] Z. Otwinowsky, W. Minor, Methods in Enzymology, in: C.W. Carter, R.M. Sweet (Eds.) vol. 276, Academic Press, New York, 1997, p. 307.
[35] Bruker, APEX2 (Version 2.1-4), SAINT (Version 7.34A), SADABS (Version 2007/4), BrukerAXS Inc, Madison, Wisconsin, USA, 2007.
[36] (a) A. Altomare, C. Burla, M. Camalli, G.L. Cascarano, C. Giacovazzo, A. Guagliardi, A.G.G. Moliterni, G. Polidori, R. Spagna, J. Appl. Cryst. 32 (1999) 115;
(b) A. Altomare, G.L. Cascarano, C. Giacovazzo, A. Guagliardi, J. Appl. Cryst. 26 (1993) 343.
[37] G.M. Sheldrick, SHELXL-97, Program for the Refinement of Crystal Structures, University of Göttingen, Germany, 1997.
[38] S. Mackay, C. Edwards, A. Henderson, C. Gilmore, N. Stewart, K. Shankland, A. Donald, MaXus: a Computer Program for the Solution and Refinement of Crystal Structures from Diffraction Data, University of Glasgow, Scotland, 1997.
[39] D. Waasmaier, A. Kirfel, Acta Cryst. A 51 (1995) 416.
[40] D. Pandiarajan, R. Ramesh, Y. Liu, R. Suresh, Inorg. Chem. Commun. 33 (2013) 33.
[41] M.M. Tamizh, B.F.T. Cooper, C.L.B. Macdonald, R. Karvembu, Inorg. Chim. Acta 394 (2013) 393.
[42] S.K. Gupta, P.B. Hitchcock, Y.S. Kushwah, G.S. Argal, Inorg. Chim. Acta 360 (2007) 2145.
[43] S. Das, S. Pal, J. Organomet. Chem. 691 (2006) 2575.
[44] X.W. Liu, J.L. Shi, J.B. Wei, C. Yang, J.X. Yan, K. Peng, L. Dai, C.G. Li, B.Q. Wang, Z.J. Shi, Chem. Commun. 51 (2015) 4599.
[45] J. Dutta, M.G. Richmond, S. Bhattacharya, Dalton Trans. 44 (2015) 13615.
[46] P.B. White, J.N. Jaworski, C.G. Fry, B.S. Dolinar, I.A. Guzei, S.S. Stahl, J. Am. Chem. Soc. 138 (2016) 4869.
[47] J. Yu, J. Liu, G. Shi, C. Shao, Y. Zhang, Angew. Chem. Int. 127 (2015) 4151.